# ARTICLE

Two Bisligand-Coordinated Luminescent Zn(II)-Coordination Polymers for Sensing of Ions and Pesticides in Aqueous Solutions

Zhao-Di Zhou[1], Zi-Long Xu[1], Dan Wang[1], Lin-Fang Jia[1], Han-Qing Zhao[1], Bao-Yi Yu[1]* and Chong-Chen Wang[2]*

[1]*Key Laboratory of Urban Agriculture (North China), Ministry of Agriculture, College of Bioscience and Resources Environment, Beijing University of Agriculture, Beijing 102206, China*

[2]*Beijing Key Laboratory of Functional Materials for Building Structure and Environment Remediation, Beijing University of Civil Engineering and Architecture, Beijing 100044, China*

ABSTRACT Two coordination polymers (CPs) $[Zn(PTA)(DTP)(H_2O)_2]\cdot(DMF)$ (**CP-1**) and $[Zn(BTC)(DTP)]\cdot(CH_3CN)_{1.5}\cdot(H_2O)_4$ (**CP-2**) with one- and two-dimensional architectures were synthesized from Zn(II) ion and different organic linkers like terephthalic acid (H_2PTA), benzene-1,3,5-tricarboxylic acid (H_3BTC), and 3,5-di(1,2,4-triazol-1-yl) pyridine (DTP). The fluorescent sensing experiments showed that the two CPs displayed effective, sensitive, and selective abilities towards Fe^{3+} and $Cr_2O_7^{2-}$. For sensing the pesticides, **CP-1** outperforms in sensing of metamitron (MMT) and **CP-2** is ultrasensitive towards imidacloprid (IMI). The possible mechanisms involved in the quenching of the fluorescence intensity include the inner filter effect (IFE) and the fluorescence resonance energy transfer (FRET) effect.

Keywords: coordination polymer, fluorescence sensing, heavy metal ions, pesticides, X-ray crystallography
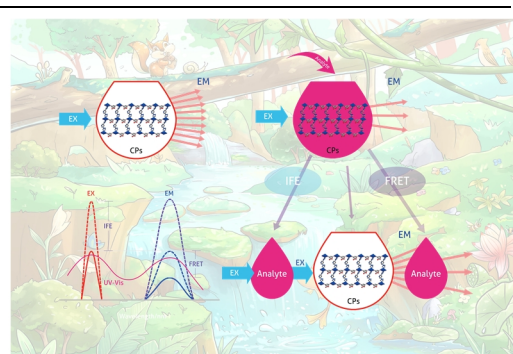
■ INTRODUCTION

Coordinated polymers (CPs), which are built up by metal centers and organic linkers through coordination bonds, have become a popular research topic during the past decade.[1-3] The exchangeable metal sites, diversified organic components and tunable architectures enable CPs to possess specific intricate chemical and physical properties like a high specific surface area, tailorable porosity, high stability and excellent functionality. These superior properties make CPs the rapidly expanding materials of interest with a wide range of applications, such as gas storage[4] and separation,[5] adsorption,[6] catalysis,[7,8] magnetic materials,[9,10] luminophores,[11] electronics,[12] and photoluminescence.[13] Luminescent CPs are an important branch of CPs. The exploration of luminescent CPs has primarily been focused on the chemical sensing, including cations,[14,15] anions,[16,17] antibiotics,[18,19] pesticides,[20] bioactive molecules,[21] amino acids,[22] pH values,[23] and temperatures.[24] Typically, the luminescent emission of CPs can arise from organic ligands and/or metal cores.[11] For organic ligands-based emission, the photoluminescence was emitted by π-electron-rich aromatic ligands or neighboring ligands via an intra- or inter-ligand charge transfer process.[11,25,26] Another case is emissive metal ion-based CPs, for instance, the most commonly used lanthanide ions based luminescent CPs,[25] which can transport the absorbed energy via a ligand-to-metal charge transfer process. Therefore, organic ligands play fundamental roles not only in the excitation and emission of photoluminescence but also in the diverse architectures of a luminescent CP. Typically, organic ligands feature *N*-donor moieties and/or carboxylate groups.[27] To benefit the advantage of both types of functional groups, one

strategy is to construct luminescent CPs by a bis-group-containing ligand, and another one is to build luminescent CPs by using two different types of ligands bearing different functional groups.[28]

With the fast growth of economics and booming development of societies, environmental pollution seriously threatens human health and natural life.[29] An overdose or deficiency of Fe^{3+} may cause serious health problems.[30] The inorganic $Cr_2O_7^{2-}$ anion is a mutagenic and carcinogenic species that may damage DNA to induce cancers and other detrimental genetic defects.[31] Besides inorganic ions, the organic contaminants also need to be considered. Pesticides are widely used to improve the agricultural production.[32] Due to the vast types and huge usage amounts of persistent or easily degradable pesticides, the detection of residuals in the environment or agricultural products is a crucial issue.[33] Until now, pollutants have been commonly detected by use of the techniques such as atomic absorption spectrometry (AAS), inductively coupled plasma-mass spectrometry (ICP-MS), gas chromatography-mass spectrometry (GC-MS), and high-performance liquid chromatography (HPLC).[34-37] Unfortunately, these methods are often expensive, complicated, area-demanding and time-consuming. Therefore, the exploration of new techniques under easy manipulation with the advantages of short response time, low cost, and real-time monitoring capabilities is highly demand. The fluorescent detection techniques meeting such requirements have been extensively investigated.[11]

In the present work, based on the above consideration, two new 1D and 2D mixed ligand-coordinated luminescent Zn(II)-MOFs coordination polymers namely: $[Zn(PTA)(DTP)(H_2O)_2]\cdot(DMF)$ (**CP-1**) (H_2PTA = terephthalic acid, 3,5-di(1,2,4-triazol-1-yl) pyridine (DTP) and DMF = dimethylformamide) and [Zn(BTC)-

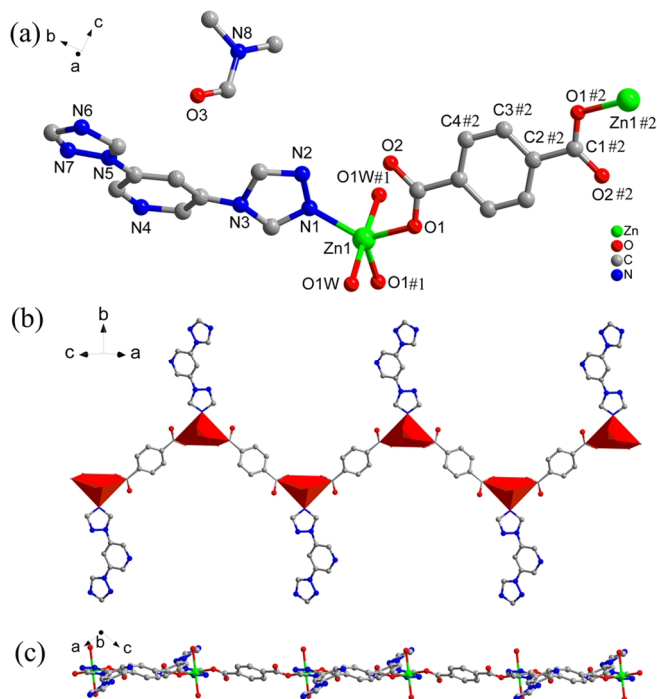**Figure 1.** (a) The coordination environment of Zn(II) ions and the ligands in **CP-1**. Symmetry codes: #1: 1 - *x*, *y*, 2.5 - *z*, #2: 0.5 - *x*, -1.5 - *y*, 3 - *z*, (b) A view of the 1D chain along the *a*-axis; (c) A view of the 1D chain along the *b*-axis.

(DTP)]·(CH$_3$CN)$_{1.5}$·(H$_2$O)$_4$ (**CP-2**) (H$_3$BTC = benzene-1,3,5-tricar-boxylate), were designed and successfully synthesized under sol-vothermal conditions. CPs with excellent fluorescent properties were employed as multi-responsive sensors. These CPs showed effective, sensitive and selective fluorescent sensing abilities to-ward inorganic ions like Fe^{3+} and Cr$_2$O$_7^{2-}$ as well as organic pesti-cide pollutants like imidacloprid (MMT) and IMI (full name). The mechanistic investigation revealed that both the inner filter effect (IFE) and the fluorescence resonance energy transfer (FRET) ef-fect are involved in the luminescent detection of inorganic ions and pesticides.

n RESULTS AND DISCUSSION

Synthesis of CPs. **CP-1** with 61% yield based on DTP ligand was prepared from Zn^{2+} and mixed organic linkers like DTP and H$_2$PTA in a mixed solvent of DMF and water (*v*/*v* = 1:1). **CP-2** was ob-tained from the reaction between Zn^{2+} and the mixture of DTP/H$_3$BTC ligands in acetonitrile and water (*v*/*v* = 1:1) solution (71% yield based on DTP ligand). The air-stable colorless crystal-line solid materials **CP-1** and **CP-2** were characterized by single-crystal X-ray diffraction analysis, FTIR, PXRD, TGA and ele-mental analysis.

X-ray Crystal Structure. The structures of **CP-1** and **CP-2** were determined by X-ray single-crystal diffraction analysis and the se-lected bond lengths and bond angles for CPs are listed in Table S1. The results show that **CP-1** and **CP-2** crystallize in monoclinic *C*2/*c* (No. 15) and triclinic *P*1̄ (No. 2) space group, respectively.
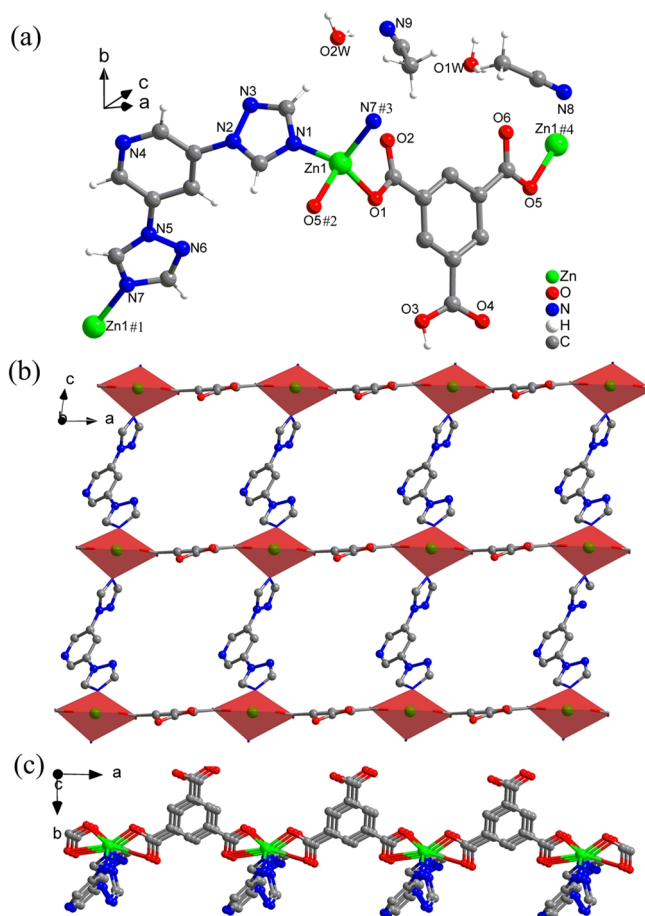

Figure 2. (a) The coordination environment of Zn(II) ions and the ligands in **CP-2**. Symmetry codes: #1: *x*, *y*, -1+*z*; #2: -1+*x*, *y*, *z*; #3: 1+*x*, *y*, 1+*z*; #4: 1+*x*, *y*, *z*. (b) A view of the 2D layer along the *a*-axis. (c) A view of the 2D layer along the *b*-axis.

The asymmetric unit of **CP-1** is composed of half-Zn(II) ion, one coordinated water molecule, half lattice DMF molecule, half DTP and half PTA ligands (Figure 1a). The unique Zn(II) center in **CP-1** is five-coordinated in a distorted hexahedral geometry by two carboxylic oxygen atoms from two PTA^{2-} ligands, one nitrogen from the DTP ligand and two oxygen atoms from two terminal wa-ter molecules. The fully deprotonated PTA^{2-} ligand serves as a two-connected linker that coordinates with two Zn(II) ions, thereby generating a "V"-shaped one-dimensional chain (Figure 1b-c).

The asymmetric unit of **CP-2** (Figure 2a) includes one Zn(II) ion, one DTP and one partially deprotonated HBTC^{2-} ligand, two lattice water molecules and two lattice acetonitrile molecules. The Zn(1) ion is four-coordinated with two carboxylic oxygen atoms from two BTC^{2-} ligands and two nitrogen atoms from two DTP ligands. This coordination environment enables the Zn(1) ion to display a dis-torted tetrahedral geometry. Both of HBTC^{2-} and DTP ligands con-nect two Zn(II) ions to form 1D chains along the *a*- and *c*-axis, respectively. Furthermore, the two chains cross each other by the Zn(II) ions to construct a double-layer 2D network (Figure 2b-c).

Characterizations. The FTIR spectra of **CP-1** and **CP-2** were an

alyzed and displayed in Figure S1. The characteristic stretching vibration peak of C=O in the protonated carboxyl group appears at approximately 1680-1700 cm^{-1},[38] which completely disappears from the profiles of the metal-containing compound **CP-1**.[39,40] However, the related peak is found in the FTIR spectrum of **CP-2** at 1700 cm^{-1} (Figure S1b) ascribed to the incomplete deprotonation of HBTC^{2-} in the process of **CP-2** formation. In addition, the asymmetric and symmetric stretching vibrations of C=O in the Zn(II)-coordinated carbonyl groups of the ligands occur at 1591 and 1370 cm^{-1} for **CP-1** and 1621 and 1347 cm^{-1} for **CP-2**. Besides FTIR analysis, the phase purities of **CP-1** and **CP-2** were evaluated by PXRD analysis. Figure S2 illustrates that the main peaks from the experiment are consistent with those of the simulated data, indicating good phase purity of the synthesized materials. In addition, the thermal stabilities of the two CPs were determined by TGA under a N$_2$ atmosphere from ambient temperature to 800 ℃ (10 ℃ min^{-1}). As shown in Figure S3, the first weight loss of **CP-1** at 20.5% (calcd. 19.8%) from room temperature to 200 ℃ corresponds to the loss of coordinated water and lattice DMF molecules. The temperature for sharp weight loss occurred at 270 ℃ due to the collapse of the skeleton of **CP-1**. For **CP-2**, an initial weight loss of 13.5% (calcd. 14.1%) was observed from room temperature to approximately 190 ℃, which corresponds to the departure of coordinated water and lattice DMF molecules. As Figure S2 shows, for **CP-2**, a rapid mass loss was observed from the curve caused by skeleton collapse at approximately 300 ℃. Considering that the stability of as-synthesized CPs would be important parameter during the sensing of analysts in aqueous media, the CPs materials in aqueous solution under different pHs (2, 4, 6, 8, 10, 12) were evaluated at room temperature for 24 hours. Figure S4 shows that the immersed CPs exhibit PXRD patterns similar to that of the intact ones, indicating strong pH stability of the CPs materials.

Fluorescent Properties of CPs and Fluorescent Sensing Solid-State Fluorescence. CPs conjugated with d^{10}-metals and organic linkers usually exhibit excellent luminescence properties. Hence, they can be used as potential luminescent sensors. The luminescence characterizations of **CP-1** and **CP-2** were evaluated, as depicted in Figure S5, where the apexes of their emission curves are located at 322 nm. The wavelength is similar to that of the free DTP ligand, while a difference in excited wavelength is found for the two CPs, with the maxima (λ_{max}) at 302 nm for **CP-1** and 277 nm for **CP-2** nm. The emission of the two CPs can be ascribed to the electronic transition of intra-ligand $\pi \rightarrow \pi^*$ and $n \rightarrow \pi^*$ orbitals[41] of the DTP ligand within CPs.

Fluorescent Sensing. Based on the excellent fluorescence ability of the two CPs, their sensing abilities towards different metal ions and pesticides were investigated. Before the sensing process, the finely grounded sensors (2.0 mg) were ultrasonically dispersed in water (10.0 mL) for 30 minutes. Then the sensing experiments were performed by mixing the sensors suspension (0.2 mg/mL) and analytes solution (2 mM for the ions and 0.2 mM for the pesticides).

Sensing of the Cations and Anions in Water. Figure 3 shows that most of the tested ions caused negligible fluorescence

quenching of the sensors; however, when introducing Fe^{3+} and Cr$_2$O$_7$$^{2-}$, significant fluorescence quenching was observed. The quenching efficiencies (defined as 1 - I/I$_0$) caused by Fe^{3+} and Cr$_2$O$_7$$^{2-}$ are 97.4% and 96.3% for **CP-1** and 97.6% and 98.2% for **CP-2**, respectively.

Besides the fluorescence sensing analyzed at a unique concentration of different targeted pollutants, a kinetic exploration of the fluorescence quenching was further measured by titration experiments to evaluate the effect of concentration of the quenchers on fluorescence intensity of the sensors. Hence, a quenching constant value of K_{sv} was introduced by the equation Stern Volmer (SV): I$_0$/I - 1 = K_{sv}[Q], where [Q] is the molar concentration of the quencher, and I$_0$ and I represent the fluorescence intensities of the sensors in aqueous solutions without and with the presence of quencher.[42,43] Figures S6-S9 show that fluorescence intensities of the sensors decreased gradually as the concentrations of the quenchers increased. In addition, at low analyte concentrations, a linear correlation was exhibited from kinetic plots (0-0.1 mM for both Fe^{3+} and Cr$_2$O$_7$$^{2-}$). However, with continuous introduction of the quencher to the suspension of the sensor, the linear curve bent upward. The K_{sv} values calculated from the SV equation from the linear ranges of the curves are 6.98×10^3 M^{-1} for Fe^{3+} and 7.80×10^3 M^{-1} for Cr$_2$O$_7$$^{2-}$ when **CP-1** was used, and 8.10×10^3 M^{-1} for Fe^{3+} and 1.60×10^4 M^{-1} for Cr$_2$O$_7$$^{2-}$ when **CP-2** was explored as the sensor.
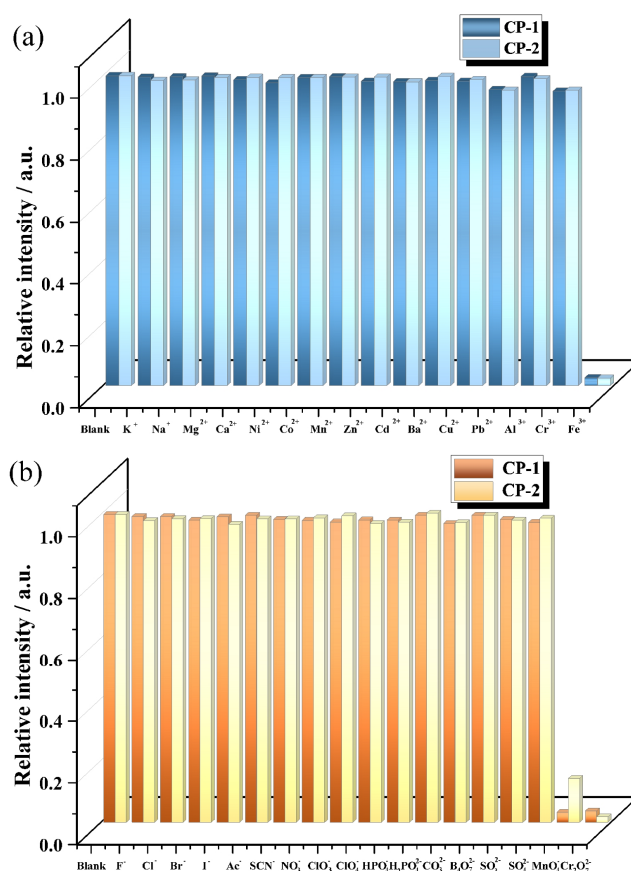

Figure 3. Quenching efficiencies of **CP-1** and **CP-2** dispersed in aqueous solutions and treated with various ions (1 mM).

In addition, another important parameter of the limit of detection (LOD) was also introduced to evaluate the sensors. The LOD equation is defined as $3\sigma/K_{sv}$ (here, σ is the relative standard error counted from ten repeated measurements of the sensor in aqueous suspensions). During fluorescent evaluation of **CP-1**, the calculated LOD values are 1.10×10^{-6} M for Fe^{3+} and 9.80×10^{-7} M for $Cr_2O_7^{2-}$ (Table S2); when using **CP-2** as the sensor, the corresponding values are 9.44×10^{-7} M for Fe^{3+} and 4.77×10^{-7} M for $Cr_2O_7^{2-}$.

Sensing of the Pesticides in Water. The excellent performance of CPs in fluorescent sensing of the ions encouraged us to further explore their applications in the detection of pesticides. Therefore, pesticides (Table S3) DIP, PCNB, IMZ, GLY, TPN, CAR, 2,4-D, IMI, and MMT in aqueous solutions were used. Figure 4 shows that IMZ, 2,4-D, GLY, DIP, PCNB, TPN, and CAR have no significant effect on the fluorescence intensity of **CP-1**. Moderate quenching was observed when IMI was used and MMT caused the most significant drop in fluorescence intensity for **CP-1**. When employing **CP-2** as the sensor, IMZ, GLY, DIP, PCNB and TPN contributed no obvious effect on the fluorescent intensity; 2,4-D, CAR and MMT contributed a moderate quenching; and IMI gave rise to the most significant quenching of the fluorescence of **CP-2**.

Furthermore, the best sensing effects toward pesticides of MMT for **CP-1** and IMI for **CP-2** were further analyzed by kinetic titration experiments. As seen from Figures S10-S11, both **CP-1** and **CP-2** shared similarities in the process of sensing of ions, i.e. as the concentration of pesticides increased, the intensities of the fluorescence dropped significantly. The plots of Ksv values illustrate a satisfactory linear correlation in the low analyte concentration range, and the curves bent upward at higher concentrations. The calculated Ksv and LOD values are 4.76×10^4 M^{-1} and 1.61×10^{-7} M for MMT when **CP-1** was used and 3.05×10^4 M^{-1} and 2.51×10^{-7} M for IMI when **CP-2** was employed as the senor. The calculated values as compared with the reported values in the fluorescent sensing of IMI or MMT are listed in Table S4.

Recyclability and Fluorescence Stability. The recyclability and regeneration of a fluorescent sensor are considered for real applications; therefore, we further studied the recycling experiments.
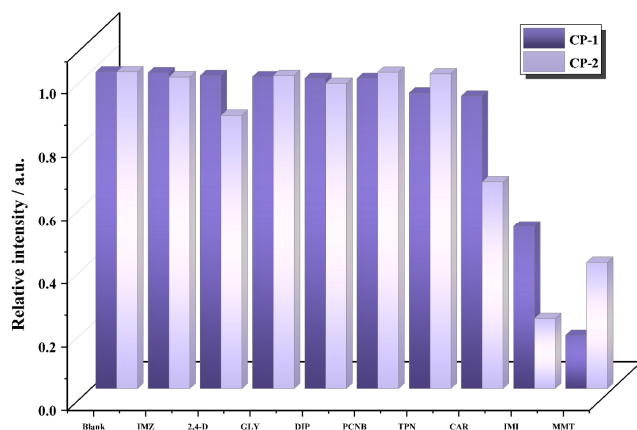

Figure 4. Quenching efficiencies of **CP-1** and **CP-2** dispersed in aqueous solutions and treated with various pesticides (0.1 mM).
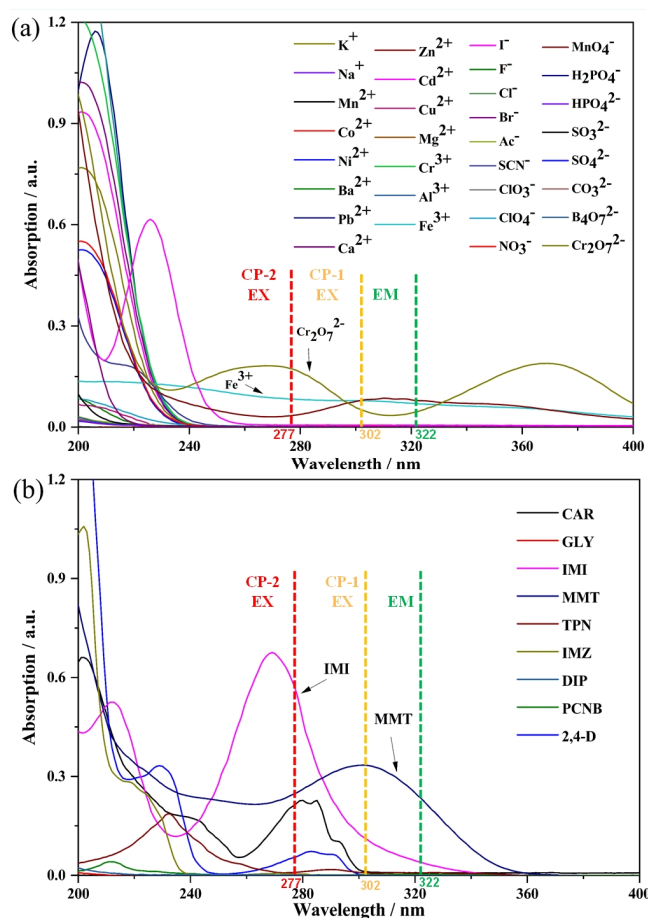

Figure 5. UV-Vis absorption spectra of different ions (a) and pesticides (b).

After recording fluorescence with or without the presence of analyte, the sensing materials were regenerated by simple centrifugation and washing with deionized water. As shown in Figure S12, there was no significant drop in the initial intensity even after five cycles of application, indicating good reusability of the sensing materials. Furthermore, fluorescence stability of the sensors under different pH conditions was also checked. Figure S13 exhibits a fluorescence summit at pH around 7. However, a slight drop of initial fluorescence intensity of the sensor was observed in case of increase or decrease of pH of the suspension. In addition, the sensors' stability with the presence of different cations and anions was also evaluated. After the sensing process of CPs for the salts, the suspensions were kept for additional 24 hours. There was no obvious appearance of transformation for both CPs under microscope. And, the single crystals of CPs under different conditions were also evaluated by using X-ray diffraction analysis (5 single crystals were analyzed for each sample), finding no change of the unit cells for the two CPs. Thereby, both CPs are stable under the tested conditions.

Possible Mechanisms for Luminescent Sensing. Regarding the exploration of possible mechanisms involved in luminescent quenching during sensing of the analytes, attention was firstly focused on the structural transformation of the sensors.[44] Accord-

ingly, FTIR (Figure S14) and PXRD (Figure S15) of **CP-1** and **CP-2** were investigated and evaluated before and after the fluorescent sensing processes, and the well-matched curves in both spectra indicated that their frameworks remained intact. Next, considering energy transformation,[45,46] the UV-Vis absorption spectra of the analytes were evaluated and illustrated together with the excitation and emission of **CP-1** and **CP-2**. As shown from Figure 5, there is strong absorption at wavelength of 277, 302, and 322 nm by both Fe^{3+} and $Cr_2O_7^{2-}$, and the UV-Vis absorption of the quenchers overlapped with both the excitation and emission light of **CP-1** and **CP-2**. The same result occurred when pesticides MMT and IMI were used. An obvious superposition between the UV-Vis absorption of the quenchers and the excitation and emission spectra of the related sensors was observed, indicating that both IFE and FRET mechanisms played key roles in reducing the fluorescent intensity of the sensors in dynamic process of the low analyte concentration range. When raising the concentration of analytes, the dynamic curves bent upward, indicating the involvement of a static mechanism occurred, which showed an interaction between analyte and the sensor.[47]

n CONCLUSION

Two mixed ligand-coordinated 1D and 2D Zn-based CPs were fabricated and characterized. The configuration of these CPs was confirmed by using single-crystal X-ray diffraction analysis. The CPs exhibited excellent fluorescence properties. Both sensors displayed extra sensitive and selective properties toward Fe^{3+} and $Cr_2O_7^{2-}$ during sensing, but **CP-1** outperformed the sensing of IMI, and **CP-2** was preferably sensitive toward MMT during sensing. Considering the involved mechanisms of the fluorescent quenching processes, IFE and FRET mechanisms were believed to play dominant roles. This work demonstrated and provided fluorescent CPs that could be used as potential fluorescent sensors to detect environmental pollutants.

n EXPERIMENTAL

Materials and Methods. All the materials and solvents were obtained commercially and used without further purification. $ZnSO_4\cdot7H_2O$, H_2PTA, H_3BTC, DMF and acetonitrile were commercially available from Aladdin. DTP was synthesized following a reported method.[48] Powder X-ray diffraction (PXRD) measurements were performed using a Bruker-Avance X-ray diffractometer equipped with a Cu-target tube and a graphite monochromator scanning over the range of 5-50° at the rate of 0.2 °/s. The simulated X-ray diffraction patterns were generated from properly treated cif files of the related CPs crystals by using the Mercury software. Elemental analyses for C, H, and N were carried out using a Perkin-Elmer 240 CHN elemental analyzer. The Fourier transform infrared (FTIR) spectrum was obtained using an Agilent Cary630 spectrophotometer in the range of 4000 to 500 cm^{-1}. UV-Vis spectroscopic studies were carried out using a Varian UV50 Conc spectrophotometer. All luminescence measurements were performed using an Agilent Cary Eclipse fluorescence spectrophotometer at room temperature. A Mettler Toledo 1600TH thermal analyzer was used to record TG curves at a heating rate of 10 °C/min in a flowing nitrogen atmosphere of 10 mL/min using platinum crucibles over the temperature range from room temperature to 800 °C.

X-ray Structure Determination. Single crystals suitable for X-ray analysis of CPs were selected and mounted on a Bruker APEX-II CCD diffractometer at 150.0(1) K during data collection using a Mo-Kα radiation (λ = 0.71073 Å). Integration and scaling of intensity data were performed by using SAINT program.[49] Data were corrected for the effects of absorption using SADABS.[50,51] Using Olex 2,[52] the structures were solved with the SIR 2004 structure solution program[53] by direct methods. Further, the structures were refined with ShelXL refinement package[54] using least-squares minimization. Non-hydrogen atoms were anisotropically refined and the hydrogen atoms in the riding mode and isotropic temperature factors were fixed at 1.2 times U(eq) of the parent atoms (1.5 times for methyl groups). For $C_{20}H_{22}N_8O_7Zn$ (**CP-1**) (CCDC 2082190) (M_r = 551.82 g/mol): monoclinic $C2/c$ space group, a = 12.9809(19), b = 14.6111(19), c = 12.3777(19) Å, β = 101.852(4)°, V = 2297.6(6) Å^3, Z = 4, T = 150.0(1) K, μ(Mo$K\alpha$) = 1.130 mm^{-1}, D_c = 1.595 g/cm^3, 11147 reflections measured (4.25≤ 2θ≤49.43°), 1962 unique (R_{int} = 0.1190, R_{sigma} = 0.0768) which were used in all calculations. The final R_1 = 0.1746 (I > 2σ(I)) and wR_2 = 0.3401 (all data). For $C_{42}H_{29}N_{17}O_{14}Zn_2$ (**CP-2**) (CCDC 2131062) (M_r = 1126.56 g/mol): triclinic system, space group $P\bar{1}$, a = 10.1370(13), b = 10.9499(14), c = 11.7439(16) Å, β = 82.503(4)°, V = 1152.0(3) Å^3, Z = 1, T = 150.0(1) K, μ(Mo$K\alpha$) = 1.129 mm^{-1}, D_c = 1.624 g/cm^3, 12177 reflections measured (3.91≤2θ≤52.92°), 4684 unique (R_{int} = 0.0843, R_{sigma} = 0.1162) which were used in all calculations. The final R_1 = 0.1511 (I > 2σ(I)) and wR_2 = 0.2552 (all data).

Fluorescence Sensing Analyses. Quenching test with unique concentration: Before the fluorescence sensing analysis, a stock solution of well-dispersed Zn-CP suspension (0.2 mg/mL) and different analyte solutions (2 mmol/mL) were prepared. Thereafter, equal volumes of the suspension and the analyte solution were mixed in a cuvette and ultrasonicated for 5 minutes. Afterwards, the resulting mixture was excited by UV light with wavelength of 302 nm for **CP-1** and 277 nm for **CP-2**, and the intensities of the emitted light were recorded at a wavelength of 322 nm for both CPs. The used analytes included the following cations (2 mM): MCl_{1-3} (M = K$^+$, Na$^+$, Mg^{2+}, Ca^{2+}, Ni^{2+}, Co^{2+}, Mn^{2+}, Cu^{2+}, Zn^{2+}, Cd^{2+}, Pb^{2+}, Ba^{2+}, Al^{3+}, Cr^{3+} and Fe^{3+}); anions (2 mM): $K_{1-2}X$ (X = F$^-$, Cl$^-$, Br$^-$, I$^-$, Ac$^-$, SCN$^-$, NO$_3^-$, ClO$_3^-$, ClO$_4^-$, HPO$_4^{2-}$, H$_2$PO$_4^-$, CO$_3^{2-}$, B$_4$O$_7^{2-}$, SO$_3^{2-}$, SO$_4^{2-}$ and Cr$_2$O$_7^{2-}$); and pesticides (0.2 mM): (dipterex, DIP; pentachloro-nitrobenzene, PCNB; imazalil, IMZ; glyphosate, GLY; chlorothalonil, TPN; carbendazim, CAR; 2.4-dichlorophenoxyacetic acid, 2,4-D; imidacloprid, IMI and metamitron, MMT). The used time for each measurement during the fluorescent sensing process is less than 30 seconds.

Luminescence kinetic titration: Before the kinetic quenching analysis, the well-mashed CP (1 mg) was added to water (10 mL), and the mixtures were stirred under ultrasonic conditions for 30 minutes. Before each fluorescent sensing measurement, aliquots (2 to 10 μL) of analytes' stock solution (20 mM for the ions and 5 mM for the pesticide) were injected into and well vortexed with the sensor suspension (4 mL).

Recyclability of Luminescence Experiments. The suspended solid CP material was centrifuged after recording the fluorescence of the blank sample in aqueous solution. Thereafter, the sediment was mixed with the analyst solution under ultrasonic conditions for 5 minutes, and the resulting mixture was subjected to a fluorescent sensing test. Then, the suspension was centrifuged again and rinsed several times with deionized water. Following the typical procedure, the experiments were repeated for an additional 4 cycles.

n ACKNOWLEDGEMENTS

n AUTHOR INFORMATION

Corresponding authors. Emails: yubaoyi123@hotmail.com and chongchenwang@126.com

n COMPETING INTERESTS

The authors declare no competing interests.

n ADDITIONAL INFORMATION

Supplementary information is available for this paper at http://manu30.magtech.com.cn/jghx/EN/10.14102/j.cnki.0254-5861.2022-0077

For submission: https://www.editorialmanager.com/cjschem

n REFERENCES

(1) Stock, N.; Biswas, S. Synthesis of metal-organic frameworks (MOFs): routes to various MOF topologies, morphologies, and composites. *Chem. Rev.* **2012**, 112, 933-969.

(2) Carlucci, L.; Ciani, G.; Proserpio, D. M.; Mitina, T. G.; Blatov, V. A. Entangled two-dimensional coordination networks: a general survey. *Chem. Rev.* **2014**, 114, 7557-7580.

(3) Murray, L. J.; Dincă, M.; Long, J. R. Hydrogen storage in metal-organic frameworks. *Chem. Soc. Rev.* **2009**, 38, 1294-1314.

(4) Kumar, K. V.; Preuss, K.; Titirici, M. M.; Rodriguez-Reinoso, F. Nanoporous materials for the onboard storage of natural gas. *Chem. Rev.* **2017**, 117, 1796-1825.

(5) Qian, Q.; Asinger, P. A.; Lee, M. J.; Han, G.; Mizrahi Rodriguez, K.; Lin, S.; Benedetti, F. M.; Wu, A. X.; Chi, W. S.; Smith, Z. P. MOF-based membranes for gas separations. *Chem. Rev.* **2020**, 120, 8161-8266.

(6) Burtch, N. C.; Jasuja, H.; Walton, K. S. Water stability and adsorption in metal-organic frameworks. *Chem. Rev.* **2014**, 114, 10575-10612.

(7) Bavykina, A.; Kolobov, N.; Khan, I. S.; Bau, J. A.; Ramirez, A.; Gascon, J. Metal-organic frameworks in heterogeneous catalysis: recent progress, new trends, and future perspectives. *Chem. Rev.* **2020**, 120, 8468-8535.

(8) Zhang, X. H.; Han, L. X.; Sheng, H. C.; Wang, S. Y. Direct catalytic nitrogen oxide removal using thermal, electrical or solar energy. *Chin. Chem. Lett.* **2022**, 33, 1117-1130.

(9) Chakraborty, G.; Park, I. H.; Medishetty, R.; Vittal, J. J. Two-dimensional metal-organic framework materials: synthesis, structures, properties and applications. *Chem. Rev.* **2021**, 121, 3751- 3891.

(10) Nartey, K. A.; Hu, J. S.; Li, J. X. Two coordination polymers with high selectivity for sensing iron(III) constructed from bifunctional ligand. *Chin. J. Struct. Chem.* **2021**, 40, 465-472.

(11) Liu, Y.; Xie, X. Y.; Cheng, C.; Shao, Z. S.; Wang, H. S. Strategies to fabricate metal-organic framework (MOF)-based luminescent sensing platforms. *J. Mater. Chem. C* **2019**, 7, 10743-10763.

(12) Sappia, L. D.; Tuninetti, J. S.; Ceolin, M.; Knoll, W.; Rafti, M.; Azzaroni, O. MOF@PEDOT composite films for impedimetric pesticide sensors. *Glob. Chall.* **2020**, 4, 1900076.

(13) Olorunyomi, J. F.; Geh, S. T.; Caruso, R. A.; Doherty, C. M. Metal-organic frameworks for chemical sensing devices. *Mater. Horiz.* **2021**, 8, 2387-2419.

(14) Fu, C.; Sun, X.; Zhang, G.; Shi, P.; Cui, P. Porphyrin-based metal-organic framework probe: highly selective and sensitive fluorescent turn-on sensor for M^{3+} (Al^{3+}, Cr^{3+}, and Fe^{3+}) ions. *Inorg. Chem.* **2021**, 60, 1116-1123.

(15) Zhai, L. J.; Tong, R.; Wang, C. B.; Shi, M. J.; Mo, Y. N.; Che, W. K.; Niu, Y. L.; Hu, T. P. Structural diversity and magnetic properties of two coordination polymers based on 6-(3,5-dicarboxylphenyl)-nicotinic acid. *Chin. J. Struct. Chem.* **2021**, 40, 1687-1695.

(16) Safaei, S.; Wang, J.; Junk, P. C. Incorporation of thiazolothiazole fluorophores into a MOF structure: a highly luminescent Zn(II)-based MOF as a selective and reversible sensor for $Cr_2O_7^{2-}$ and MnO_4^- anions. *J. Solid State Chem.* **2021**, 294, 121762.

(17) Zhang, Y. Q.; Sheng, S. S.; Mao, S.; Wu, X. H.; Li, Z.; Tao, W. Q.; Jenkinsond, I. R. Highly sensitive and selective fluorescent detection of phosphate in water environment by a functionalized coordination polymer. *Water Res.* **2019**, 163, 114883.

(18) Yuan, R.; He, H. State of the art methods and challenges of luminescent metal-organic frameworks for antibiotic detection. *Inorg. Chem. Front.* **2020**, 7, 4293-4319.

(19) Wang, C. Y.; Wang, C. C.; Zhang, X. W.; Ren, X. Y.; Yu, B. Y.; Wang P.; Zhao, Z. X.; Fu, H. F. A new Eu-MOF for ratiometrically fluorescent detection toward quinolone antibiotics and selective detection toward tetracycline antibiotics. *Chin. Chem. Lett.* **2022**, 33, 1353-1357.

(20) Zhou, Z. D.; Wang, C. Y.; Zhu, G. S.; Du, B.; Yu, B. Y.; Wang, C. C. Water-stable europium(III) and terbium(III)-metal organic frameworks as fluorescent sensors to detect ions, antibiotics and pesticides in aqueous solutions. *J. Mol. Struct.* **2022**, 1251, 132009.

(21) Dong, J.; Zhao, D.; Lu, Y.; Sun, W. Y. Photoluminescent metal-organic frameworks and their application for sensing biomolecules. *J. Mater. Chem. A* **2019**, 7, 22744-22767.

(22) Guo, W. X.; Wang, Y. Y.; Hu, X. L.; Qi, Y.; Gao, E. Q. Homochiral helical coordination architectures built from biphenyl based amino acid derivatives: structural diversity tuned by varying conformation and configuration of N-donor ligands, sensing of acidic amino acids, and photoluminescence properties. *Cryst. Growth Des.* **2020**, 20, 5072-5085.

(23) Yang, S. L.; Li, G.; Guo, M. Y.; Liu, W. S.; Bu, R.; Gao, E. Q. Positive cooperative protonation of a metal-organic framework: pH-responsive fluorescence and proton conduction. *J. Am. Chem. Soc.* **2021**, 143, 8838-8848.

(24) Mukhopadhyay, A.; Jindal, S.; Savitha, G.; Moorthy, J. N. Temperature-dependent emission and turn-off fluorescence sensing of hazardous "quat" herbicides in water by a Zn-MOF based on a semi-rigid dibenzochrysene tetraacetic acid linker. *Inorg. Chem.* **2020**, 59, 6202-6213.

(25) Yan, B. Luminescence response mode and chemical sensing mechanism for lanthanide-functionalized metal-organic framework hybrids. *Inorg. Chem. Front.* **2021**, 8, 201-233.

(26) Xing, S.; Janiak, C. Design and properties of multiple-emitter lumine-

scent metal-organic frameworks. *Chem. Commun.* **2020**, 56, 12290-12306.

(27) Yang, H.; Qi, D.; Chen, Z.; Cao, M.; Deng, Y.; Liu, Z.; Shao, C.; Yang, L. A Zn-based metal-organic framework as bifunctional chemosensor for the detection of nitrobenzene and Fe^{3+}. *J. Solid State Chem.* **2021**, 296, 121970.

(28) Gosselin, A. J.; Rowland, C. A.; Bloch, E. D. Permanently microporous metal-organic polyhedra. *Chem. Rev.* **2020**, 120, 8987-9014.

(29) Ding, M.; Yang, Y.; Duan, X.; Wang, S.; Feng, X.; Wang, T.; Wang, P.; Liu, S.; Li, L.; Liu, J.; Tang, L.; Niu, X.; Zhang, Y.; Li, G.; Yao, W.; Cui, L.; Wang, W. Association of genetic polymorphisms of telomere binding proteins with cholinesterase activity in omethoate-exposed workers. *Ecotoxicol. Environ. Saf.* **2018**, 161, 563-568.

(30) Wu, K.; Hu, J.; Shi, S.; Li, J.; Cheng, X. A thermal stable pincer-MOF with high selective and sensitive nitro explosive TNP, metal ion Fe^{3+} and pH sensing in aqueous solution. *Dyes Pigm.* **2020**, 173, 107993.

(31) van Heerden, P. V.; Jenkins, I. R.; Woods, W. P. D.; Rossi, E.; Cameron, P. D. Death by tanning - a case of fatal basic chromium sulphate poisoning. *Intens. Care Med.* **1994**, 20, 145-147.

(32) Elfikrie, N.; Ho, Y. B.; Zaidon, S. Z.; Juahir, H.; Tan, E. S. S. Occurrence of pesticides in surface water, pesticides removal efficiency in drinking water treatment plant and potential health risk to consumers in Tengi River Basin, Malaysia. *Sci. Total Environ.* **2020**, 712, 136540.

(33) Lykogianni, M.; Bempelou, E.; Karamaouna, F.; Aliferis, K. A. Do pesticides promote or hinder sustainability in agriculture? The challenge of sustainable use of pesticides in modern agriculture. *Sci. Total Environ.* **2021**, 795, 148625.

(34) Håkansson, K.; Coorey, R. V.; Zubarev, R. A.; Talrose, V. L.; Håkansson, P. Low-mass ions observed in plasma desorption mass spectrometry of high explosives. *J. Mass Spectrom.* **2000**, 35, 337-346.

(35) Moros, J.; Laserna, J. J. New Raman-laser-induced breakdown spectroscopy identity of explosives using parametric data fusion on an integrated sensing platform. *Anal. Chem.* **2011**, 83, 6275- 6285.

(36) Moreno-González, D.; Lara, F. J.; Jurgovská, N.; Gámiz-Gracia, L.; García-Campaña, A. M. Determination of aminoglycosides in honey by capillary electrophoresis tandem mass spectrometry and extraction with molecularly imprinted polymers. *Anal. Chim. Acta* **2015**, 891, 321-328.

(37) Tabrizchi, M.; Ilbeigi, V. Detection of explosives by positive corona discharge ion mobility spectrometry. *J. Hazard. Mater.* **2010**, 176, 692-696.

(38) Ju, P.; Yang, H.; Jiang, L.; Li, M.; Yu, Y.; Zhang, E. A novel high sensitive Cd-MOF fluorescent probe for acetone vapor in air and picric acid in water: synthesis, structure and sensing properties. *Spectrochim. Acta A Mol. Biomol. Spectrosc.* **2021**, 246, 118962.

(39) Qin, G.; Wang, J.; Li, L.; Yuan, F.; Zha, Q.; Bai, W.; Ni, Y. Highly water-stable Cd-MOF/Tb^{3+} ultrathin fluorescence nanosheets for ultrasensitive and selective detection of cefixime. *Talanta* **2021**, 221, 121421.

(40) Liu, Y. K.; Zhou, X. H. Synthesis, structure and property of a metal-organic framework based on 9-(2,6-dicarboxy-pyridin-4-yl)-9H-carbazole-3,6-dicarboxylic acid. *Chin. J. Struct. Chem.* **2020**, 39, 559-566.

(41) Feng, D.; Tang, J.; Yang, J.; Ma, X.; Fan, C.; Wang, X. A multiresponsive luminescent probe of antibiotics, pesticides, Fe^{3+} and ascorbic acid with a cadmium(II) metal-organic framework. *J. Mol. Struct.* **2020**, 1221, 128841.

(42) Li, C.; Yang, W.; Zhang, X.; Han, Y.; Tang, W.; Yue, T.; Li, Z. A 3D hierarchical dual-metal-organic framework heterostructure up-regulating the pre-concentration effect for ultrasensitive fluorescence detection of tetracycline antibiotics. *J. Mater. Chem. C* **2020**, 8, 2054-2064.

(43) Pan, M. Q.; Yang, R. Q.; Muhammad, Y.; Cai, K. T.; Han, F.; Zhang, H. C.; Niu, Y. Q.; Wang, H. Crystal structure, Fe^{3+} luminescence sensing and color tuning of 2D lanthanide-metal-organic frameworks constructed from tricarboxylic acid ligand. *Chin. J. Struct. Chem.* **2022**, 41, 2202023-2202033.

(44) Feng, L.; Wang, K. Y.; Day, G. S.; Ryder, M. R.; Zhou, H. C. Destruction of metal-organic frameworks: positive and negative aspects of stability and lability. *Chem. Rev.* **2020**, 120, 13087-13133.

(45) Chen, S.; Yu, Y. L.; Wang, J. H. Inner filter effect-based fluorescent sensing systems: a review. *Anal. Chim. Acta* **2018**, 999, 13-26.

(46) Jin, Y.; Zhang, Q.; Zhang, Y.; Duan, C. Electron transfer in the confined environments of metal-organic coordination supramolecular systems. *Chem. Soc. Rev.* **2020**, 49, 5561-5600.

(47) Lakowicz, J. R. *Principles of Fluorescence Spectroscopy.* 3rd ed.; Springer: New York **2006**

(48) Wang, C. L.; Song, C. Q.; Shen, W. H.; Qi, Y. Y.; Xue, Y.; Shi, Y. C.; Yu, H.; Feng, L. A two-dimensional Ni(II) coordination polymer based on a 3,5-bis(1′,2′,4′-triazol-1′-yl)pyridine ligand for water electro-oxidation. *Catal. Sci. Technol.* **2019**, 9, 1769-1773.

(49) Madison, W. I. SAINT, ver. 8.40A, Bruker Nano **2019**.

(50) Madison, W. I. SADABS, ver. 2016/2, Bruker AXS **2016**.

(51) Krause, L.; Herbst-Irmer, R.; Sheldrick, G. M.; Stalke, D. Comparison of silver and molybdenum microfocus X-ray sources for single-crystal structure determination. *J. Appl. Crystallogr.* **2015**, 48, 3-10.

(52) Dolomanov, O. V.; Bourhis, L. J.; Gildea, R. J.; Howard, J. A. K.; Puschmann, H. OLEX2: a complete structure solution, refinement and analysis program. *J. Appl. Crystallogr.* **2009**, 42, 339-341.

(53) Burla, M. C.; Caliandro, R.; Camalli, M.; Carrozzini, B.; Cascarano, G. L.; De Caro, L.; Siliqi, D.; Polidori, G.; Spagna, R.; Giacovazzo, C. IL MILIONE: a suite of computer programs for crystal structure solution of proteins. *J. Appl. Crystallogr.* **2007**, 40, 609-613.

(54) Sheldrick, G. SHELXT - Integrated space-group and crystal-structure determination. *Acta Crystallogr., Sect. A* **2015**, 71, 3-8.